13th World Conference on Earthquake Engineering
Vancouver, B.C., Canada
August 1-6, 2004
Paper No. 1285

JSSI MANUAL FOR BUILDING PASSIVE CONTROL TECHNOLOGY PART-12 VELOCITY-DEPENDENT DAMPER PERFORMANCE UNDER EXTREMELY SMALL EXCITATION

Yoji OOKI[1], Kazuhiko KASAI[2], Osamu TAKAHASHI[3] and Yohei SEKIGUCHI[4]

SUMMARY

This paper reports the experimental result of the velocity-dependent damper under extremely small responses. The dampers used for the experiment were three oil dampers and one viscoelastic (VE) damper, and each damper was tested using the shaking table connected a mass in series. The dampers show the responses of about 0.1-0.5 mm because the response magnification of the testing system is very small. Although the properties of the VE damper was almost equal to the standard value provided by the manufacturer, those values of the oil dampers differ. The oil dampers are usually modeled by Maxwell element with a set of the dashpot and the spring, and the properties of the model were found to have velocity sensitivity.

INTRODUCTION

Velocity-dependent dampers such as oil dampers or viscoelastic dampers have been applied to many buildings as seismic control devices and they are installed to the structures through braces in general. (Tsuyuki [1]) These dampers are expected to improve habitability of buildings by reducing small vibration in these days. To live up to this expectation, the dampers should work effectively not only for seismic excitation. Performance experiments of velocity-dependent damper under small excitation have been reported by Ikahata [2], Sunakoda [3] and Inoue [4], but these experiments target only one example and have not been studied qualitatively. Therefore the performance of the damper under small excitation has not figured out clearly yet. Especially about mechanical device such as oil damper which consists piston and cylinder, it is needed to validate the performance of actual damper under small excitation since mechanical gaps or friction resistance at the joints or inside of the damper are at risk of reducing the damper performance in that condition.

[1] Research Assoc., Structural Engineering Research Center, Tokyo Institute of Technology, Yokohama, Japan.
[2] Prof., Structural Engineering Research Center, Tokyo Institute of Technology, Ph.D., Yokohama, Japan.
[3] Chief Engineer, Kozo Keikaku Engineering Inc., Tokyo, Japan.
[4] Kozo Keikaku Engineering Inc., Tokyo, Japan.

In general, performance of velocity-dependent damper is considered with dependency of equivalent stiffness K_d' and equivalent viscosity C_d' on circular frequency ω of excitation as shown in Figs. 1 and 2. Time history analysis model of oil damper is represented by Maxwell body which consists a spring with internal stiffness K_d and a dashpot with internal viscosity C_d in series, and the equivalent stiffness and the equivalent viscosity are represented as shown in Eq. (1).

$$K_d' = \frac{K_d (C_d \omega)^2}{K_d^2 + (C_d \omega)^2} \quad , \qquad C_d' = \frac{K_d^2 C_d}{K_d^2 + (C_d \omega)^2} \tag{1}$$

On the other hand, time history analysis model of viscoelastic damper is represented by Kelvin body whose spring has the equivalent stiffness K_d' and dashpot has the equivalent viscosity C_d' with dependency on frequency. (Kasai [5]) It seems to be valid to evaluate the performance of damper under small excitation with the equivalent K_d' and the equivalent viscosity C_d' under sinusoidal excitation, moreover with the internal stiffness K_d and the internal viscosity C_d for oil damper. This paper reports the sinusoidal excitation experiment for actual dampers under extremely small excitation in detail, which had not almost been reported before. The amplitude of the response varies from 0.1 to 0.5 mm. The dampers used in this experiment are three oil dampers with 500 kN capacity offered by three different manufacturers, and a viscoelastic damper.

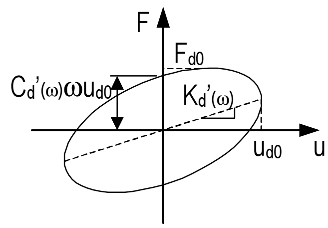

Fig. 1 Hysteresis Loop of Sinusoidal Response

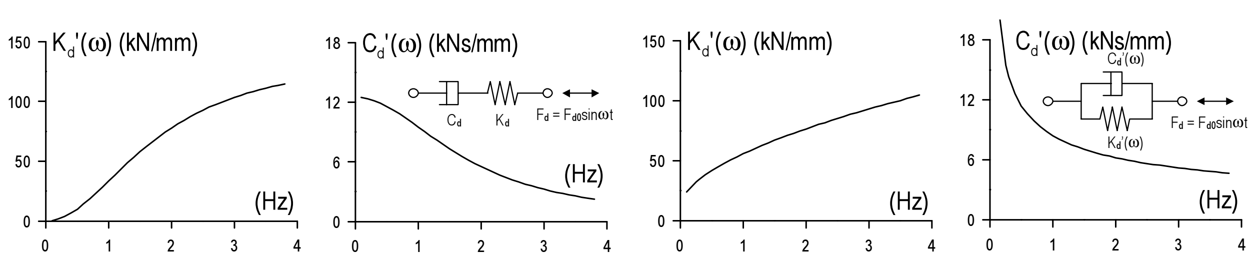

(a) Oil Damper **(b) Viscoelastic Damper**

Fig. 2 Dependency of Damper on Frequency of Sinusoidal Response

SUMMARY OF EXPERIMENT

Test Method and Dampers

A shaking table was used for the experiment of sinusoidal excitation. Fig. 3 shows the testing machine with damper, which constrains the horizontal response to be unidirectional. This experiment is equivalent to controlling the load into damper since this testing system is single mass system with a mass connected to damper directly and the input acceleration acts on the mass. Furthermore, since the frequency of the excitation is less than the resonance frequency of the system, the response displacement magnification factor of the damper becomes very small as 1/1,000 to 1/10 (0.25 to 3 Hz). And it makes the system possible to give small amplitude to the damper by shaking the shaking table with large and stable amplitude. This system was adopted since actuators with large capacity, which are used in common shaking test for velocity-dependent dampers, cannot control small amplitude.

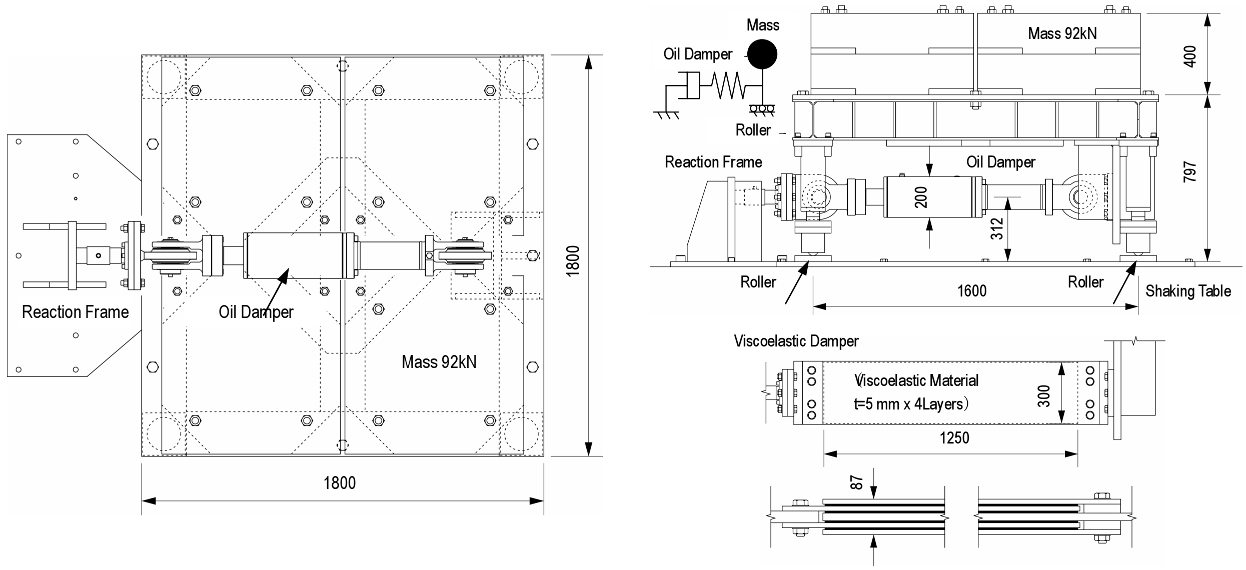

Fig. 3 Testing Machine and Dampers

Three oil dampers (Damper-A, B, C) are for seismic control and have the same internal stiffness K_d and internal viscosity C_d as shown in Table 1. Since the specification may vary under small amplitude, it is necessary to verify the applicable range for each oil damper. (JSSI [6]) The basic composition of oil damper is shown in appendix A. On the other hand, the thickness and the shear area of the viscoelastic damper (Damper-D) are decided as the response amplitude to be equal to one of oil damper. The dependency of the equivalent stiffness K_d' and the equivalent viscosity C_d' of the dampers on frequency is shown in Fig. 2.

Table 1 Specification of Dampers

Damper Type	Equivalent Values (1Hz, 20°C)	Specification
Oil	K_d' = 33.5 kN/mm C_d' = 9.5 kN·s/mm, η_d = 1.8	K_d = 140 kN/mm C_d = 12.5 kN·s/mm
Viscoelastic	K_d' = 55.8 kN/mm C_d' = 8.4 kN·s/mm, η_d = 1.0	A_s = 1.5 m^2, d = 5 mm

A_s: Shear Area, d: Thickness of Viscoelastic Material

Measurement and Shaking Plan

Fig. 4 represents the measurement plan on this experiment. The characters in the figure represent displacement (deformation) as D, acceleration as A and temperature as T. The damper force shown in this paper was obtained as the output of the load cell LC, and the damper stroke is obtained as the average of the output of the displacement meter, and which is represented as (D3 + D4) / 2.

Fig. 5 represents the shaking plan of the experiment. Input wave takes five kinds of frequency and four kinds of maximum velocity of shaking table for each damper. The input displacement of shaking table was increased gradually to avoid rapid increase of response amplitude and deviation of the load.

Table 2 shows the sampling settings for the measurement, and it was decided as the number of data in a period to be 333 (for 1.5 and 3 Hz) or 400 (for 0.25, 0.5 and 1 Hz).

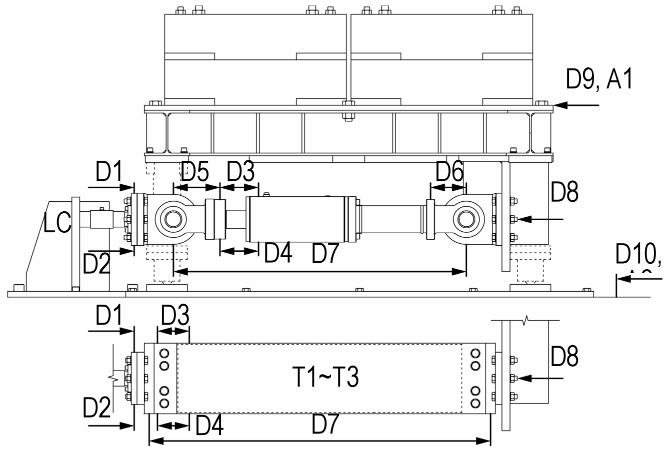

Fig. 4 Measurement Plan

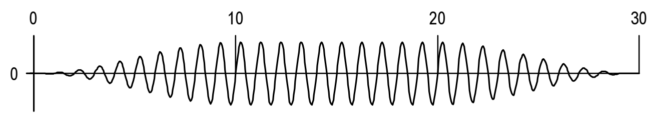

Shaking Frequency (Hz)	0.25, 0.5, 1, 1.5, 3
Maximum Velocity of Shaking Table (cm/s)	10, 20, 30, 40

Fig. 5 Shaking Plan

Table 2 Sampling Settings for Data Collection

Shaking Frequency (Hz)	0.25	0.5	1	1.5	3
Sampling Frequency (Hz)	100	200	400	500	1000
Number of Data in a Period	400			333	

Identification of Characteristics

However the performance of the damper should be evaluated including the effect of mechanical gaps of the pins at the both ends, this paper only evaluate the damper stroke as the response amplitude to make the point clear. The effect of the gaps is shown in appendix B.

This paragraph shows how to identify the characteristics of the damper, the equivalent stiffness K_d' and the equivalent viscosity C_d'. In general, the hysteresis loop of the results of shaking test has some irregularities according to the input noise especially under small excitation, and it is necessary to remove those disorders as much as possible on identifying the characteristics of the dampers. In this paper, the equivalent stiffness is obtained recursively with least-square method, which obtains the linear function $F_{di} = K_d' \cdot u_{di}$ with n values of deformation u_{di} and damper force F_{di}.

$$K_d{}' = \frac{n\left(\sum_i u_{di} F_{di}\right) - \left(\sum_i u_{di}\right)\left(\sum_i F_{di}\right)}{n\left(\sum_i u_{di}{}^2\right) - \left(\sum_i u_{di}\right)^2} \tag{2}$$

On the other hand, the equivalent viscosity is obtained with absorbed energy E_d in a stable hysteresis loop regarded as a sinusoidal response as shown in Eq. (3) where u_{d0} represents the maximum response amplitude and ω represents the circular frequency of the excitation.

$$C_d' = E_d / (\pi \cdot \omega \cdot u_{d0}^2) \tag{3}$$

Furthermore, the internal stiffness K_d and the internal viscosity C_d of oil damper are obtained as shown in Eqs. (4). Eq. (4a) represents loss factor η_d.

$$\eta_d = C_d' \cdot \omega / K_d' \tag{4a}$$
$$K_d = K_d' \ (1 + \eta_d^2) \tag{4b}$$
$$C_d = C_d' \ (1 + \eta_d^2) / \eta_d^2 \tag{4c}$$

The internal stiffness K_d, is often obtained by dividing the maximum damper force by the instant deformation due to its simplicity. (Tsuyuki [7]). However this is difficult to evaluate the internal stiffness precisely even with stable sinusoidal response since the deformation increases rapidly at the maximum damper force. Furthermore, noise of experiment makes it more difficult, so this is not proper way to evaluate the precise values.

RESULTS OF EXPERIMENT

Hysteresis Characteristics

The solid lines in Fig. 6 represent relationship between damper force and damper stroke at the fifth cycle of the steady-state shaking. They are smoothed by moving-average method with eleven smoothing points. The dashed lines represent the results of numerical analysis with the characteristics which have been obtained by the way described above. The analysis models are modeled as Maxwell body for oil damper (Takahashi [8]) and Kelvin body for the viscoelastic damper.

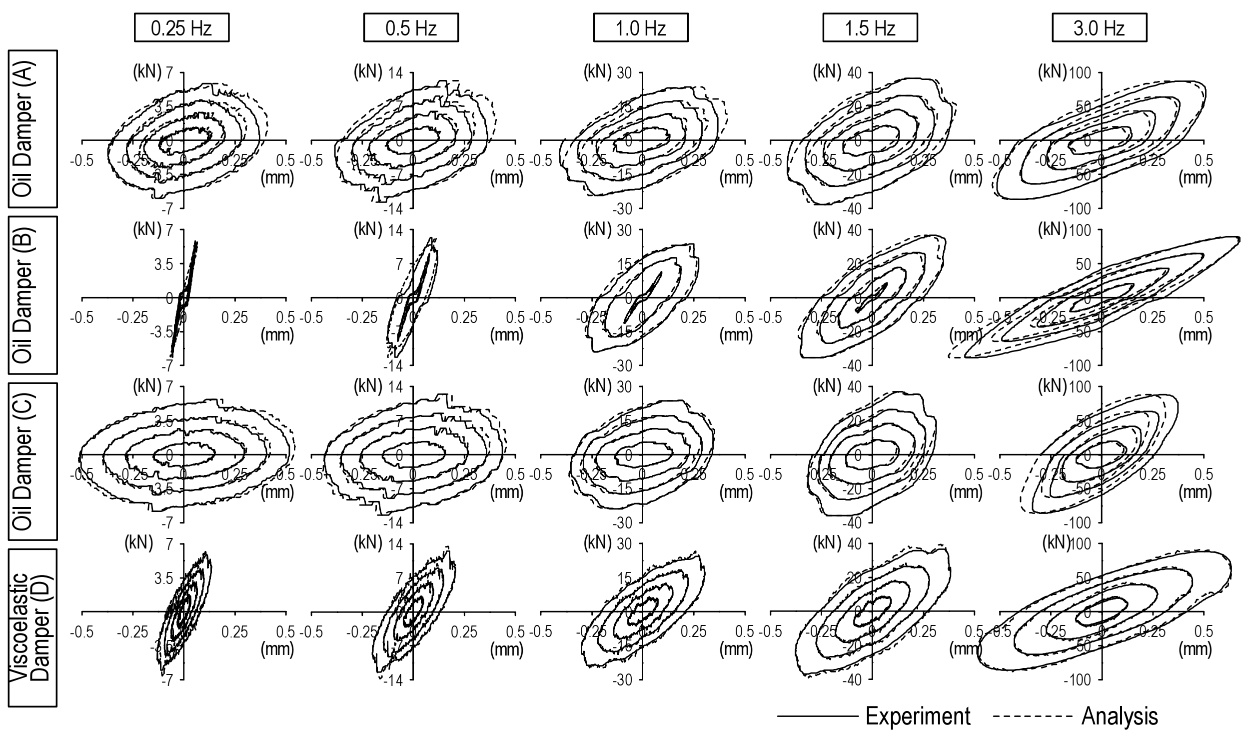

Fig. 6 Sinusoidal Responses

The hysteresis loops have irregularities by the noise of input acceleration to the mass, which affect the damper force, since the input to the damper is the load transmitted by the mass connected in series. Especially, the responses under 3 Hz excitation show almost bi-linear hysteresis loops since the input acceleration are not precise sinusoidal waves due to the capability of the shaking table. However, the results of the numerical analysis shown as dashed lines accord with those of the experiment well including the irregularities by the disorder of the input. That is to say, the identification of the characteristics shown by the proposed equations Eqs. (2) to (4) is valid.

The absorbed energy of Damper-B is small since the stiffness under small excitation is larger than those of the other oil dampers and the response amplitude becomes small. The damper force of Damper-B larger than 10 kN is stable in this experiment. The slender hysteresis loops of Damper-B will be mentioned later. Besides, the hysteresis loops were expected to be rectangle by frictional force, but they are not. The next section describes the further studies about the dependency of the equivalent stiffness K_d' and the equivalent viscosity C_d' on frequency, amplitude and velocity.

Equivalent Stiffness K_d' and Equivalent Viscosity C_d'

Fig. 7 shows the dependency of the equivalent stiffness K_d' and the equivalent viscosity C_d', which was obtained as described in the previous section, on frequency of excitation, damper stroke and stroke velocity of damper. The dashed lines in the figure represents the standard values of K_d' and C_d' calculated with the specification shown in Table 1. They are obtained by Eq. (1) for oil damper, and analysis model or evaluation equations shown by manufacturers for viscoelastic damper in general. (Kasai [9], Hanzawa [10] and KKE [11])

Although the equivalent stiffness K_d' of Damper-A accord with the dependency of Maxwell body on frequency, the equivalent viscosity C_d' takes about 5 to 8 kN·s/mm and has wide dispersion below 1.5 Hz. Besides, the more the stroke velocity gets larger, the less the dispersion of the results of the experiment increases. On the other hand, although both the equivalent stiffness K_d' and the equivalent viscosity C_d' of Damper-B accord with the model, they have dispersion under low frequency especially the equivalent viscosity C_d'. Furthermore, the behavior of Damper-C is not much different from one of Damper-A, but the equivalent stiffness K_d' is less wholly.

At the same time, the results of the experiment of viscoelastic damper Damper-D accord with the model well. However this viscoelastic damper is just an example, it seems to have the damper performance as the standards even under extremely small excitation since the structure of viscoelastic damper is simpler than one of oil damper.

As above, the characteristics of oil dampers under small excitation differ from the standards and that tendency varies by each damper. The next section studies the internal stiffness K_d and the internal Viscosity C_d of Maxwell body of oil dampers.

Internal Stiffness K_d and Internal Stiffness C_d of Maxwell Body

Fig. 8 shows the dependency of the internal stiffness K_d and the internal viscosity C_d of Maxwell body for oil damper on frequency of excitation, damper stroke and stroke velocity. The dashed lines in the figure represents the standards of K_d and C_d as shown in Table 1 and they should be independent on any of frequency of excitation, damper stroke and stroke velocity as well as they might have been.

The results of all three dampers converge as the increase of the stroke velocity. While the equivalent stiffness K_d of Damper-D almost accords with the standards, one of Damper-A becomes 1.68 times and one of Damper-C becomes 2.68 times of the standards. Meanwhile, the internal viscosity C_d converges in 0.87, 1.24, 1.25 times of the standards for Damper-A, B, C in order.

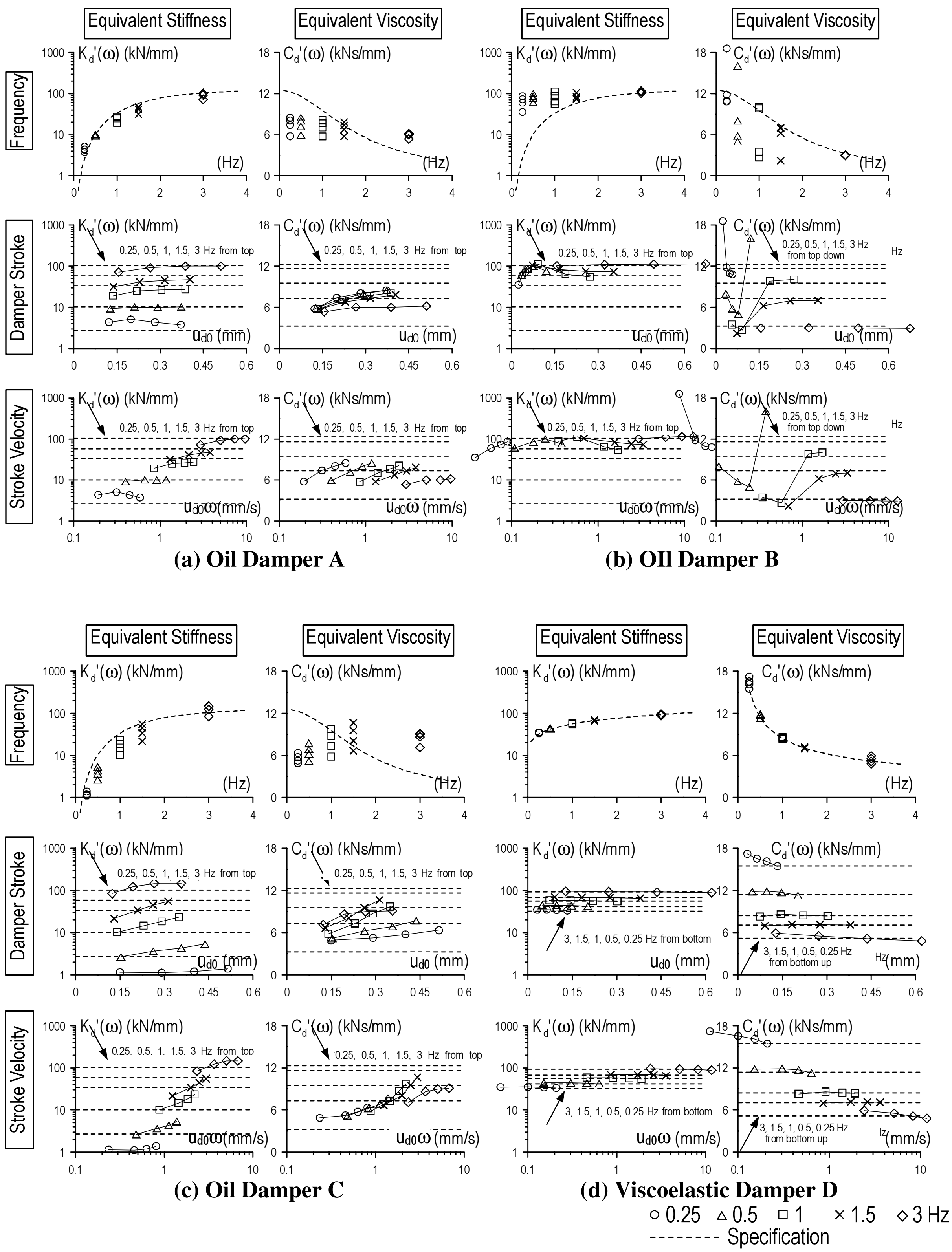

Fig. 7 Equivalent Stiffness and Equivalent Viscosity

Under low velocity and low frequency, the internal stiffness K_d takes much less than the standards for all dampers, and the internal viscosity C_d takes less for Damper-A and C and much larger for Damper-B. Fig, 9 represents the sinusoidal response as shown in Fig. 6 before, and this shows that K_d and C_d identified by Eq. (2) to (4) make the hysteresis loop to absorb energy little. This results from that the deformation concentrates at spring by decrease of deformation of the dashpot as increase of the internal viscosity C_d of Maxwell body.

Maximum Damper Force and Absorbed Energy

This section studies the relationship between the maximum damper force F_{d0} and the velocity of excitation, which is represented as stroke velocity $u_{d0}\cdot\omega$, and the absorbed energy E_d by the evaluation method of performance test which manufacturers do for the linear response. (Kasai [9]) While this evaluation method evaluates both the equivalent viscosity C_d' and the absorbed energy, only the absorbed energy is considered here.

Fig. 10 represents the relationships between the maximum damper force F_{d0} and the maximum damper stroke u_{d0}, and the maximum stroke velocity $u_{d0}\cdot\omega$ for each damper. The dashed lines in the figure represent the theoretical solutions of the damper stroke and the stroke velocity of the excitation, and they are obtained with the equivalent stiffness K_d' and the equivalent viscosity C_d' which are calculated by applying the internal stiffness K_d and the internal viscosity C_d, shown in Table 1, to Eq. (1).

$$u_{d0} = \frac{F_{d0}}{\sqrt{K_d'^2 + (C_d'\omega)^2}} \tag{5}$$

The maximum damper force of Damper-A and C are clearly less than the standards under 0.25 and 0.5 Hz, and larger than them under 3 Hz. This is realized that the characteristics of these dampers exceed the standards under frequency below about 1.5 Hz as shown in Fig. 6. On the other hand, the damper force of Damper-B exceeds the standards in all cases especially under 0.25 Hz. This is not by the damping performance but by that the equivalent stiffness K_d' is extremely large as shown in Fig. 7. In this way, damping performance of damper cannot be evaluated properly with the maximum damper force since the damper force may be large even if the damper performance is short. This should be considered especially under extremely small amplitude. The maximum damper force of viscoelastic damper (Damper-D) has less error than oil dampers since the equivalent stiffness K_d' and the equivalent viscosity C_d' are about the same as the standards.

Furthermore, the relationships between the maximum damper force and the absorbed energy are shown in Fig. 11. The dashed lines in the figure represents the theoretical solutions of the absorbed energy E_d obtained from the maximum damper stroke u_{d0} in Eq. (5) and C_d' in Eq. (1).

$$\begin{aligned} E_d &= \pi(C_d'\omega)u_{d0}^2 \\ &= \pi(C_d'\omega)\frac{F_{d0}^2}{K_d'^2 + (C_d'\omega)^2} \end{aligned} \tag{6}$$

The absorbed energy of Damper-B become much less than the standards with small damper force below 10 kN, and get closer to the standards as increase of the damper force. Those of Damper A, C are almost the same as the standards in all cases although the equivalent stiffness K_d' and the equivalent viscosity C_d' don't accord with the standards as shown before. This may be described as that the entire absorbed energy becomes almost the same as the standards since u_{d0} gets large (Fig. 8 (a), (c)) under the frequency with C_d' which is less than the standards (Fig. 6 (a), (c)).

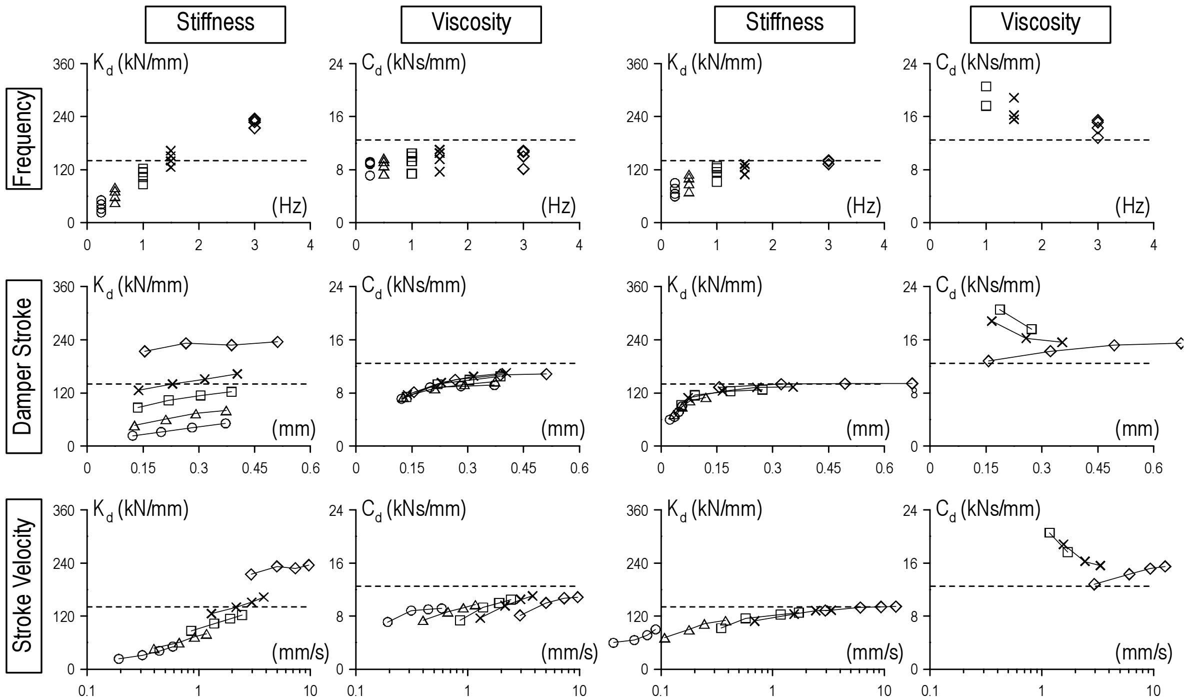

(a) Oil Damper A **(b) Oil Damper B**

Fig. 8 (a), (b) Internal Stiffness and Internal Viscosity of Maxwell Body

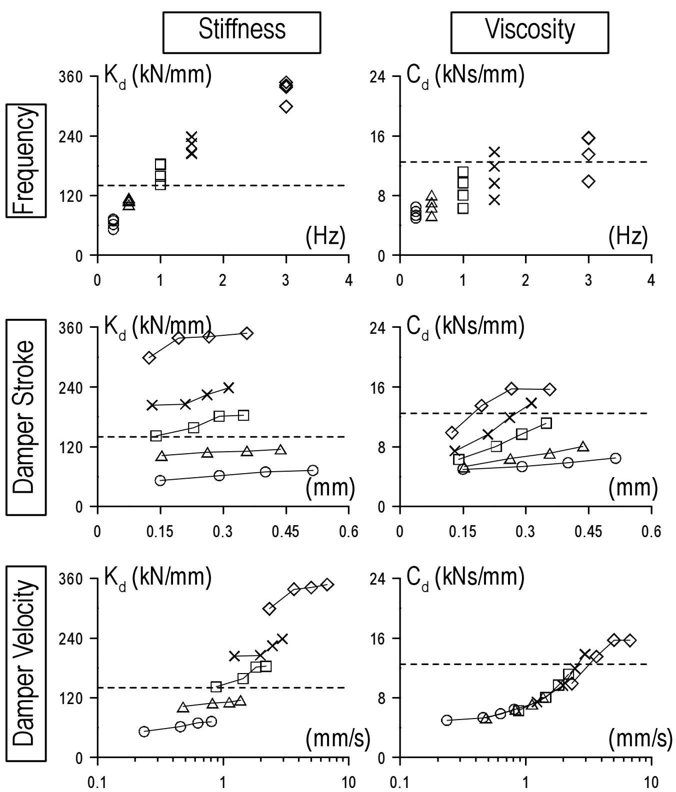

(c) Oil Damper C

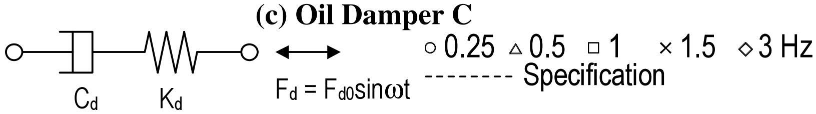

Fig. 8 (c) Internal Stiffness and Internal Viscosity of Maxwell Body

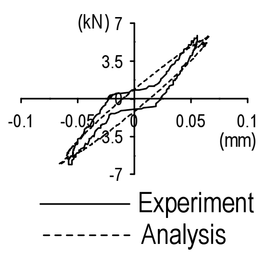

Fig. 9 Sinusoidal Response of Damper-B (0.25 Hz)

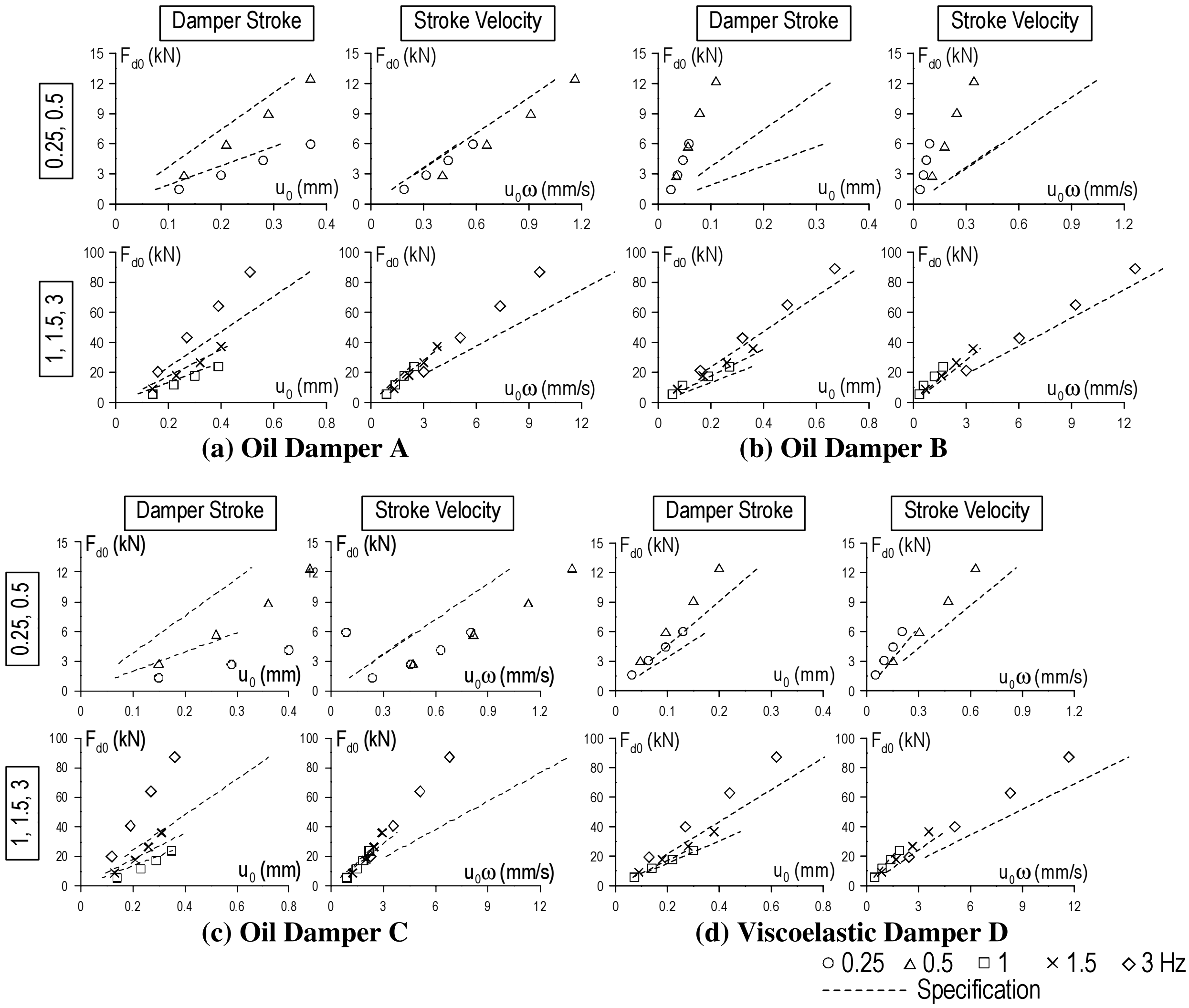

Fig. 10 Relationships between Maximum Damper Force and Damper Stroke and Stroke Velocity

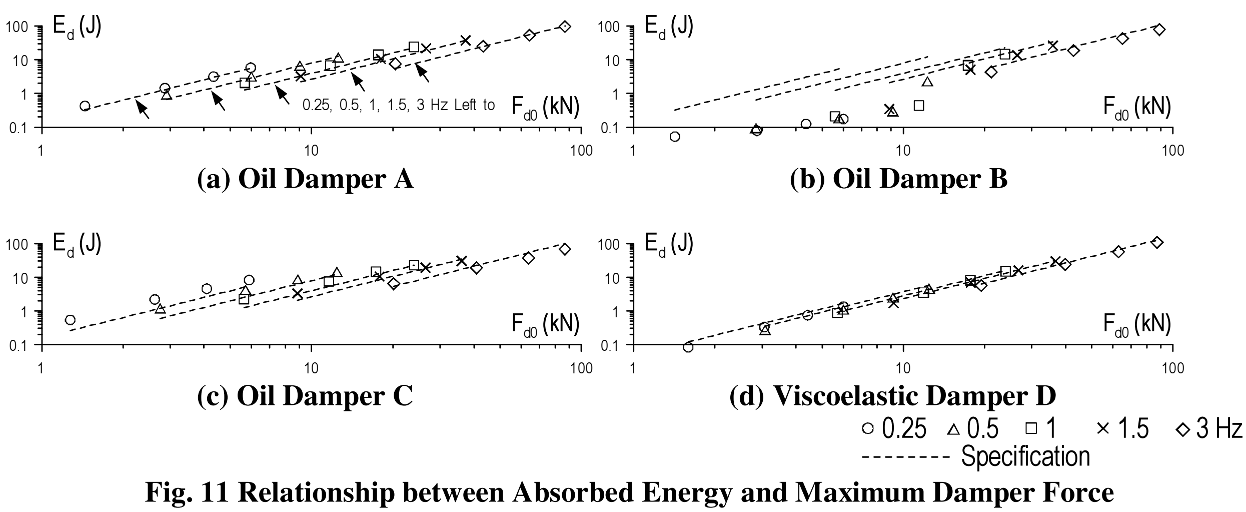

Fig. 11 Relationship between Absorbed Energy and Maximum Damper Force

CHARACTERISTICS OF OIL DAMPER UNDER EXTREMELY SMALL AMPLITUDE

Since the internal stiffness K_d and the equivalent viscosity C_d converge as the increase of the stroke velocity as described above, the sinusoidal excitations for Damper A, B were continued until the damper performance to be stable due to evaluate the dependency of these characteristics on velocity for Damper A, B. The results shown here are in the range where the relief valves of the dampers do not work.

Fig. 12 represents the internal stiffness and the internal viscosity of the damper with the stroke velocity below about 35 mm/s in addition to those of under small amplitude. The evaluation functions are obtained as the regression functions of the results under small amplitude, and the characteristics are evaluated as the average of the results under larger amplitude. The characteristics appear K_d = 203 kN/mm, C_d = 11.2 kN·s/mm for Damper-A and K_d = 131 kN/mm, C_d = 14.3 kN·s/mm for Damper-B. The internal stiffness K_d appears much larger than the specification shown in Table 1. And the regression functions are obtained as follows, where units for each variable are K_d kN/mm, C_d kN·s/mm, u_{d0} mm and ω rad/s.

Damper-A:

$$K_d = 61.9 \ln(u_{d0} \cdot \omega) + 95.5 \tag{7a}$$

$$C_d = 0.846 \ln(u_{d0} \cdot \omega) + 8.95 \tag{7b}$$

Damper-B:

$$K_d = 14.6 \ln(u_{d0} \cdot \omega) + 115 \tag{8a}$$

$$C_d = -30.8 \ln(u_{d0} \cdot \omega) + 62.6 \tag{8b}$$

Damper-C:

$$K_d = 104 \ln(u_{d0} \cdot \omega) + 143 \tag{9a}$$

$$C_d = 3.88 \ln(u_{d0} \cdot \omega) + 7.81 \tag{9b}$$

The damper performance of Damper-A, B becomes almost stable when stroke velocity is larger than about 10 mm/s. The internal viscosity C_d of Damper-B appears to be very large, but some of them seem to increase with stroke velocity as those of Damper-A. Under small velocity, the equivalent stiffness of Damper-B is large since the piston of the damper cannot move smoothly, but more smoothly the piston moves, the internal viscosity C_d may increase with stroke velocity with a speculation.

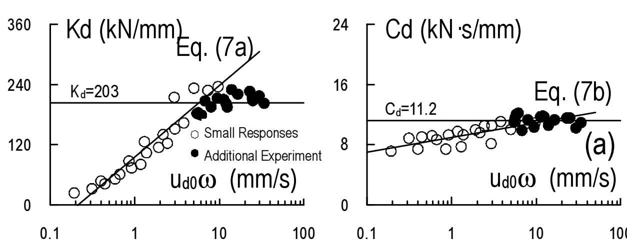

(a) Oil Damper A

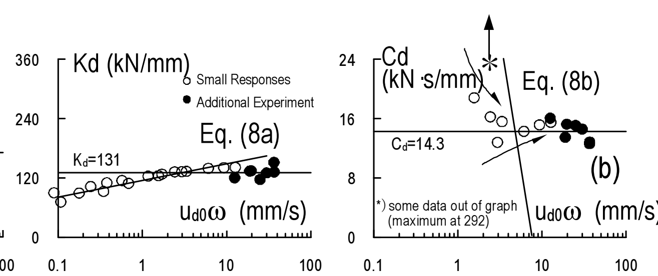

(b) Oil Damper B

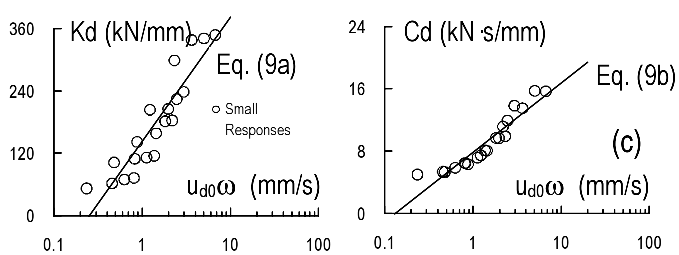

(c) Oil Damper C

Fig. 12 Evaluation of Internal Stiffness and Internal Viscosity of Oil Damper

CONCLUSIONS

The experiment for three actual oil dampers and a viscoelastic damper under sinusoidal excitation with small amplitude was taken and their characteristics were evaluated in this paper. The conclusions are shown as follows.

1) The experiment for velocity-dependent dampers of sinusoidal excitation with small amplitude was taken and the testing system with a shaking table was proposed. This system made it possible to obtain extremely small response of damper as 0.1 to 0.5 mm with stable excitation of the shaking table.
2) The identifications for the equivalent stiffness K_d' and the equivalent viscosity C_d' with the results of experiment considering the effect of noise were shown. And the time history analysis model with these characteristics accord with the results of the experiment precisely.
3) While the equivalent stiffness K_d' and the equivalent viscosity C_d' of viscoelastic damper appears to be almost the same as the standards, the internal stiffness K_d and the internal viscosity C_d of oil dampers differ from the standards and they depend on stroke velocity.
4) To evaluate the results of performance test of damper, it is to be noted that the damper force under small amplitude may accord with the standard not because of the viscous damping force but because of the elastic force by stiffness. Therefore, the internal stiffness K_d' and the internal viscosity C_d' are to be evaluated instead of the damper force.

APPENDIX

A. Basic Composition of Oil Damper

Fig. A1 represents the basic composition of oil damper. The damper force is the fluid resistance force of oil passing through the orifice and it is proportional to velocity due to the regulator. With Maxwell model, viscous damping force is represented as fluid resistance at the orifice and stiffness of spring is nearly equivalent to the compression stiffness of oil.

The regulator opens and shuts according to volume of oil flow, but if the volume is small such as under small amplitude, it cannot work normally. To avoid this problem, fixed orifice without regulator is often used in combination with it. Damper-A and C used in this experiment have this mechanism. Oil flows through the fixed orifice with small volume of flow, and through the orifice with regulator under larger volume. When the regulator works, the share of the fixed orifice gets small relatively.

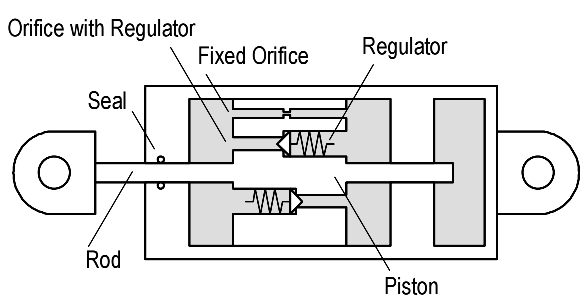

Fig. A1 Basic Composition of Oil Damper

B. Effect of Mechanical Gaps of Damper

Here shows the evaluation of the mechanical gaps of the pins at the both ends of oil damper. The gap is represented as – (D1 + D2) / 2 – D8 – (D3 + D4) / 2 (Fig. 3).

Fig. B1 represents the typical hysteresis loops of Damper-B and C under 0.5 Hz and 20 cm/s excitation. And Fig. B2 (a) represents the time histories of the damper force under this excitation. The vertical axis is normalized by the maximum force 6.1 kN. The damper force almost traces the ideal sinusoidal wave shown as dashed line. Fig. B2 (b) represents the time history of the damper stroke and the gap. The vertical axis is normalized by each maximum values. While the transition of the phase of the both gaps accord with those of the damper forces, one of the damper stroke of Damper-C differs from one of the damper force. The tangent of this phase difference is equivalent to what is called loss factor. The slenderness of the hysteresis loop of Damper-B as shown in Fig. B1 is thought to be aftereffects of that the phase difference is small and the loss factor becomes small.

The solid lines shown in Fig. B2 (c) represents the actual deformation of the damper which is evaluated as the sum of the damper stroke and the gap. The time history of the total deformation of the damper peaks at the left of one of the damper stroke and the phase difference gets smaller. This means that the mechanical gaps of the damper affect the behavior of the damper.

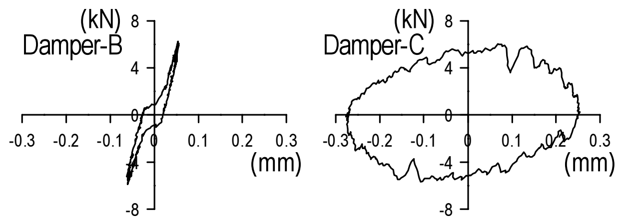

Fig. B1 Hysteresis Loop of Damper-B and Damper-C

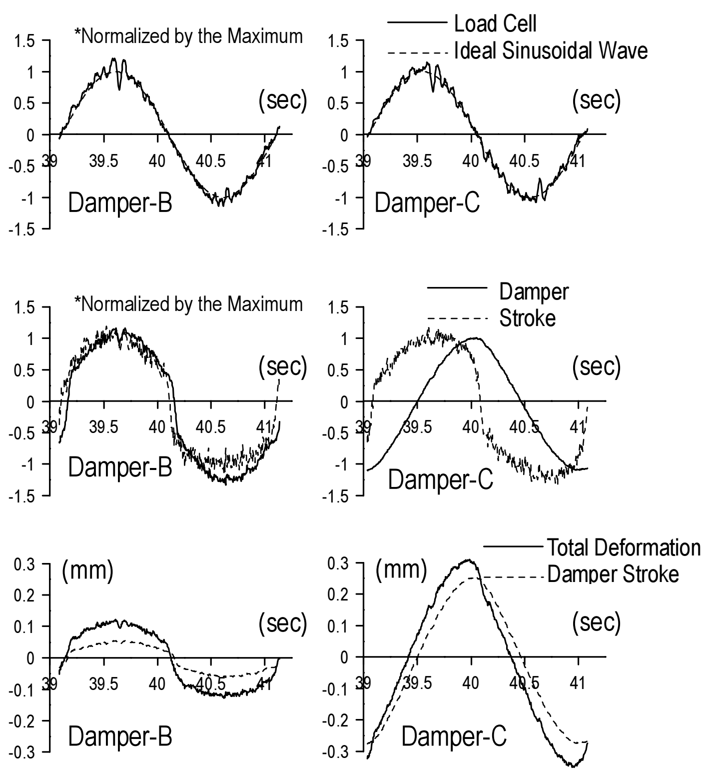

Fig. B2 Time History of Damper-B and Damper-C

REFERENCES

1. Tsuyuki Y, Ninomiya M, Takahashi O, et.al. “Development of Response-Controlled Structural System of Using Oil Damper (Part I – III)” Summaries of Technical Papers of Annual Meeting Architectural Institute of Japan 1998: 933-938.
2. Ikahata N, Shibata M, Iiyama F, Miyamoto Y, et.al. “Development of Hydraulic Damper for Minute Vibration with Loading Column (Part I – IV)” Summaries of Technical Papers of Annual Meeting Architectural Institute of Japan 2000: 847-854.
3. Sunakoda K, Ikahata N, Iiyama F, et.al. “Development of Hydraulic Damper for Minute Vibration (Part – I)” Summaries of Technical Papers of Annual Meeting Architectural Institute of Japan 1999: 1061-1062.
4. Inoue R, Shibata K, et.al. “Development of Hydraulic Damper for Minute Vibration (Part II – III)” Summaries of Technical Papers of Annual Meeting Architectural Institute of Japan 2000: 863-866.
5. Kasai K, Okuma K. “Kelvin-Type Formulation and Its Accuracy for Practical Modeling of Linear Viscoelastic Dampers” Journal of Structural and Construction Engineering (Transactions of Architectural Institute of Japan) 2001.12: 71-78.
6. “Manual for Design and Construction of Passively-Controlled Buildings” Japan Society of Seismic Isolation. 2003.
7. Tsuyuki Y, Kamei T, Gofuku Y, Iiyama F. “Performance and Quality Control of Oil Damper” Passively Controlled Structure Symposium 2001, Yokohama, Japan: 45-58.
8. Takahashi O, Sekiguchi Y. “Constitutive Rule of Oil Damper with Maxwell Model and Source Code for Analysis Program” Passively Controlled Structure Symposium 2001, Yokohama, Japan.
9. Kasai K, Teramoto M, Okuma K, Tokoro K. “Constitutive Rule for Viscoelastic Materials Considering Temperature, Frequency and Strain Sensitivities” Journal of Structural and Construction Engineering (Transactions of Architectural Institute of Japan) 2001.5: 77-86.
10. Hanzawa T, Nakamura Y, Isoda K, Sone Y. “Development of Visco-Elastic Damper with Styrene Elastomer (Part II)” Summaries of Technical Papers of Annual Meeting Architectural Institute of Japan 2002: 817-818.
11. “User’s Manual for Seismic Analysis Program for Buildings RESP-M/II” Kozo Keikaku Engineering Inc.
12. Ooki Y, Kasai K, Takahashi O. “Performance of Velocity-Dependent Dampers under Extremely Small Responses” Journal of Structural Engineering, Architectural Institute of Japan, Vol.50B 2003.